scientific reports

Check for updates

OPEN

Retinal "sweet spot" for myopia treatment

Barbara Swiatczak[1]✉, Hendrik P. N. Scholl[2,3] & Frank Schaeffel[1,4,5]

We studied which retinal area controls short-term axial eye shortening when human subjects were exposed to + 3.0D monocular defocus. A custom-built infrared eye tracker recorded the point of fixation while subjects watched a movie at a 2 m distance. The eye tracker software accessed each individual movie frame in real-time and covered the points of fixation in the movie with a uniform grey patch. Four patches were programmed: (1) foveal patch (0–3 degrees), (2) annular patch (3–9 deg), (3) foveal patch (0–3 deg) combined with an annular patch (6–9 deg), and (4) full-field patch where only 6–10 deg were exposed to the defocus. Axial eye shortening was elicited similarly with full-field positive defocus and with the foveal patch, indicating that the fovea made only a minor contribution (-11 ± 12 µm vs. -14 ± 17 µm, respectively, n.s.). In contrast, patching a 3–9 degrees annular area or fovea together with an annular area of 6–9 degrees, completely suppressed the effect when compared with full-field defocus (+ 3 ± 1 µm or -2 ± 13 µm vs. -11 ± 12 µm, respectively, $p < 0.001$). Finally, we found that the near-peripheral retina (6–10 degrees) is a "sweet spot" for positive defocus detection and alone can regulate eye growth control mechanism, and perhaps long-term refractive development (-9 ± 8 µm vs. full-field: -11 ± 12 µm, n.s.).

Keywords Retina, Defocus, Axial length, Fovea, Periphery, Emmetropization

Several studies have shown that the peripheral retina is most responsive to imposed defocus and may therefore have a major impact on emmetropization (review[1]:). The first findings came from animal models. Experiments in chickens and rhesus monkeys demonstrated that optical defocus or diffusion, imposed in the nasal hemisphere of the visual field (including the fovea) changed axial length and refractive error only in the temporal retina, suggesting that the retina controls eye growth locally[2–4]. Smith et al. showed that rhesus monkeys treated with diffusers that covered only the peripheral visual field but left central vision unrestricted, still developed longer eyes and more myopic refractive errors in the center of the visual field[5]. Further, they also showed that the development of and recovery from deprivation myopia was not altered after foveal ablation by laser photocoagulation[6,7]. Similarly, experiments in marmosets showed that imposing hyperopic defocus selectively in the peripheral retina still induced axial myopia, while imposing peripheral myopic defocus caused relative axial hyperopia, that was similar in magnitude to full-field exposure[8]. A recent experiment in infant rhesus monkeys also suggested that emmetropization may be controlled within 20 degrees from the fovea[9].

A role of the peripheral retina in emmetropization was also assumed based on electroretinogram (ERG) recordings in human subjects which showed that retinal responses strongly depend on the magnitude and the location of the imposed blur[10]. Panorgias et al. used the "dead leaves stimulus" (DLS) paradigm which was phase reversed at 7.5 Hz. ERGs were recorded while wavefront errors were simulated by digital filtering of the DLS in concentrical areas at different eccentricities. Wavefront errors ranged between 0.1 and 0.5 µm which was equivalent to about 0.2 to 1 D of unsigned defocus, depending on pupil size. ERGs were most affected by blur imposed between 6 and 12 degrees (deg) eccentricity. Interestingly, blur applied beyond 12 deg eccentricity did not alter the ERG responses while blur outside the central 6 degrees did not alter responses from full-field blur[10].

The assumption that peripheral refractive status may be associated with myopia onset and progression is currently prevalent[11,12]. It has been shown that children who became myopic had more hyperopic relative peripheral refractive error than persisting emmetropes, which could occur even before myopia onset[13,14]. However, there is no final decision as to whether peripheral refractive errors are a reason or a consequence of refractive errors[15]. Since peripheral image quality may play an important role in refractive development, a number of optical interventions were developed to alter the peripheral retinal image[16]. While an inhibitory effect on myopia was observed in all cases (DIMS[17], DOT[18,19], HAL[20], MyoCare[21]), the effects were variable and the

[1]Institute of Molecular and Clinical Ophthalmology Basel (IOB), Basel, Switzerland. [2]University of Basel, Basel, Switzerland. [3]Department of Clinical Pharmacology, Medical University of Vienna, Vienna, Austria. [4]Section of Neurobiology of the Eye, Ophthalmic Research Institute, University of Tuebingen, Tuebingen, Germany. [5]Zeiss Vision Lab, Institute of Ophthalmic Research, University of Tuebingen, Tuebingen, Germany. ✉email: barbaraswiatczak@gmail.com

reasons were not clear. Therefore, more research is needed also to map out the most responsive retinal areas and determine which types of retinal image degradation may be most effective.

Experiments in animal models have shown that visually triggered changes in eye growth start with short-term changes in choroidal thickness. Short-term changes in choroidal thickness, which can also be measured as changes in axial length[22], are assumed to predict future eye growth, and recent long-term studies in children support such an association[23,24]. Choroidal thinning (also visible as an increase in axial length) is followed by later axial elongation and myopia development, while choroidal thickening (also visible as a decrease in axial length) is associated with eye growth inhibition[2,25]. Also, studies in humans demonstrated that imposed optical defocus can rapidly change choroidal thickness and axial length in children and adult subjects[26,27].

The goal of the current study was to gain more insight as to which retinal areas generate the growth-inhibiting signals when monocular myopic defocus is imposed by a trial lens. We used a novel approach. A monocular custom-built eye tracker recorded the fixation points when subjects watched a movie on a large 65" screen at a 2 m distance. The software accessed each movie frame and covered respective areas around the fixation point with a uniform gray patch to remove local spatial information and therefore information about defocus. Four visual field patches were tested: (1) a 0–3 deg eccentricity foveal patch, (2) an annular patch covering an area between 3 and 9 deg eccentricity, (3) a 0–3 deg foveal patch combined with an annular patch covering the area between 6 and 9 deg eccentricity, and (4) full-field patch where only 6 to 10 deg of retinal eccentricity was exposed to positive defocus. The effects of imposed positive defocus with different patches of the visual field on short-term axial length change were compared with the effects of full field defocus. They were also compared with the changes induced in control fellow eyes which had normal vision during the entire experiment.

Results

Eyes convergence and gaze tracking

To ensure that all subjects had normal binocular vision and achieved continuous fusion during movie watching, a custom-built binocular eye tracker[28] was used that recorded both eye positions. Since the eye tracker involved an automated calibration procedure for both eyes at the same time, the same pixel coordinates of the fixation points on the screen would be expected for both eyes. Supplementary Figure S1 (online) shows scatter plots representing both eye positions in the horizontal and vertical directions for all subjects. The very high Pearson's correlation coefficients (horizontal and vertical axis: $R^2 = 0.99$, $p < 0.0001$) demonstrate that the fixation points of both eyes were largely superimposed in the movie plane.

An analysis of all eye positions recorded by the monocular eye tracker revealed that subjects looked mostly into the central part of the screen in the vertical and horizontal plane (Fig. 1A). The distributions of eye positions did not differ between the foveal patch, the 3–9 deg eccentricity annular patch, and the foveal patch combined with a 6–9 deg eccentricity annular patch (Fig. 1B, C, and D, respectively).

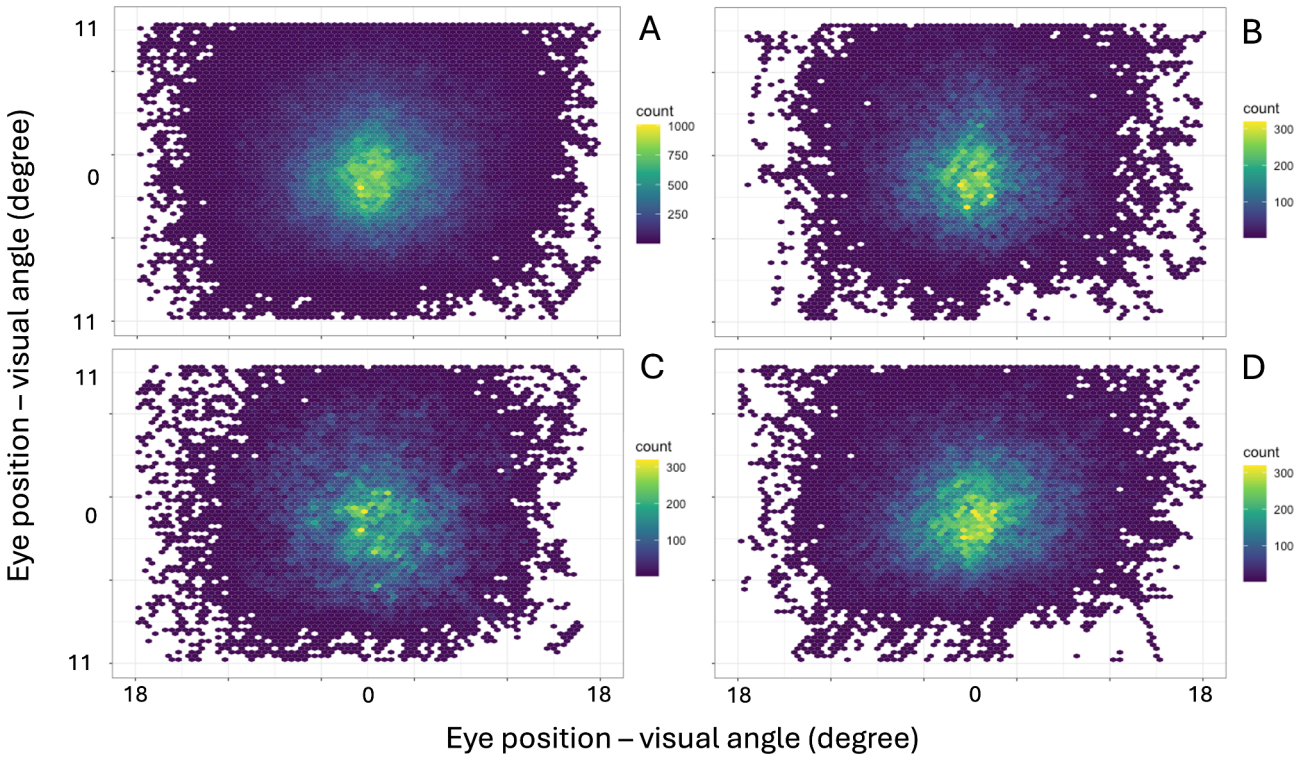

Fig. 1. Two-dimensional density plots showing the distributions of eye positions of all subjects during the entire experiment (**A**), while watching a movie with a foveal patch (**B**), a 3–9 degrees eccentricity annular patch (**C**), and a foveal patch combined with a 6–9 degrees eccentricity annular patch (**D**).

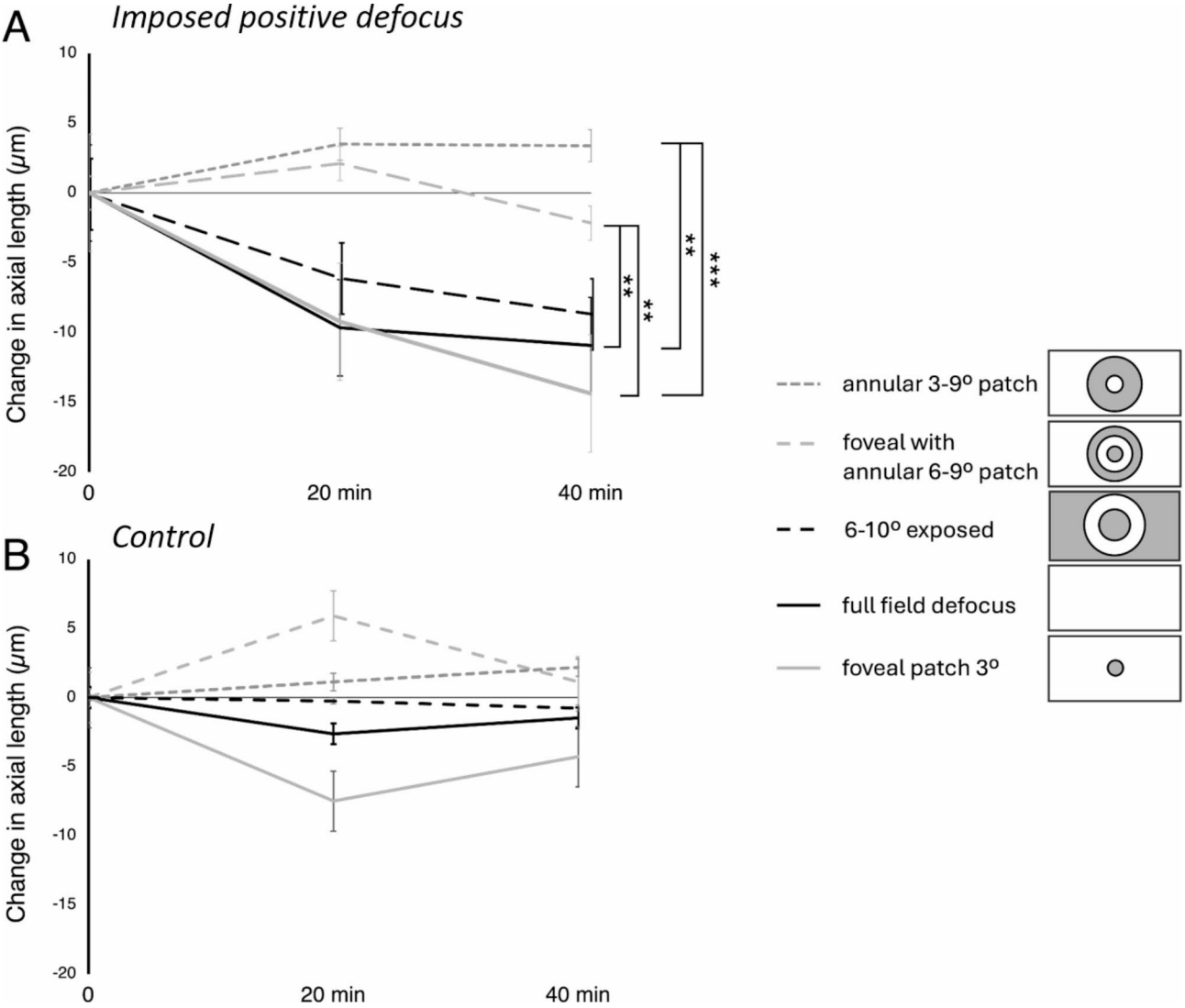

Fig. 2. (**A**) Average effects of imposed positive defocus on axial length when different parts of the visual field were covered with a gray patch: foveal patch with a radius of 3 deg (gray solid line), full-field patch with exposed 6–10 degrees annular area (black dashed line), foveal patch with a radius of 3 deg, combined with an annular patch of 6–9 deg eccentricity (bright gray dashed line), and an annular patch covering the area between 3 and 9 degrees eccentricity (dark gray dashed line). The black line represents the effect of full field defocus. (**B**) Average change in axial length after 20 and 40 min in control fellow eyes. Error bars denote SEMs. Significance levels ** $p < 0.01$, *** $p < 0.001$.

Effects of full-field defocus on axial length

Imposed positive defocus (+3.0 D) induced significant axial eye shortening after 20 min (-10 ± 14 µm, $p = 0.005$) and 40 min (-11 ± 12 µm, $p = 0.001$) compared with control, fellow eyes without the defocus (20 min: -3 ± 11 µm, 40 min: -1 ± 12 µm) and when compared to the baseline measurement (20 min: $p = 0.008$, 40 min: $p = 0.001$) (Figs. 2 and 3A).

Effects of positive defocus imposed outside the fovea

Covering the central 6 deg of the visual field (radius 3 deg) did not suppress axial eye shortening. Axial length changes did not differ from the effect of full-field defocus (20 min: -9 ± 14 µm vs. -10 ± 14 µm, 40 min: -14 ± 17 µm vs. -11 ± 12 µm, respectively, both n.s.). There was also significant axial eye shortening in defocused eyes with a patched fovea when compared with their control, fellow eyes after 40 min of stimulation (-14 ± 17 µm vs. -4 ± 9 µm, $p = 0.02$) and when compared with the baseline measurement (20 min: $p = 0.002$, 40 min: $p = 0.0002$) (Figs. 2 and 3B).

Effects of positive defocus with a 3–9 degrees eccentricity annular patch

Covering a 3–9 deg eccentricity annular area of the visual field completely diminished the effect of imposed positive defocus on axial length which was no longer different from the axial length changes induced in

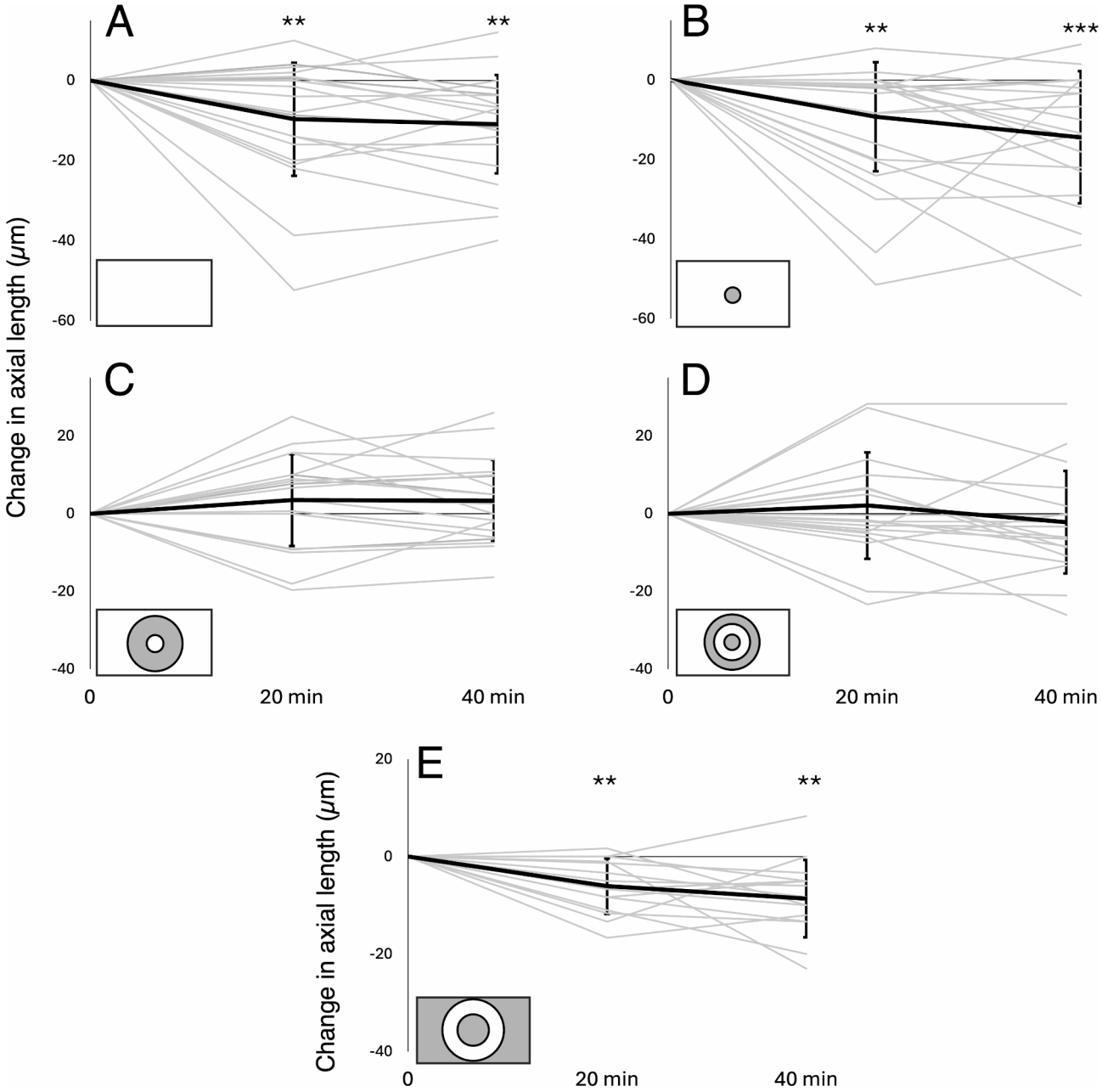

Fig. 3. Changes in axial length after exposure to positive defocus in individual subjects (gray lines) and average changes in all subjects (thick black line) recorded after 20 and 40 min relative to the baseline measurement. Error bars denote standard deviations. Significance levels: ** $p < 0.01$, *** $p < 0.001$.

control, fellow eyes at any time point (20 min: +3 ± 3 μm vs. +1 ± 10 μm, 40 min: +3 ± 11 μm vs. +2 ± 14 μm, respectively, both n.s.). However, these changes were significantly different from those induced after full-field defocus (+3 ± 11 μm vs. -11 ± 12 μm, $p = 0.0004$) (Figs. 2 and 3C).

Effects of positive defocus imposed only on the area between 3 and 6 degrees eccentricity and in the periphery beyond 9 degrees eccentricity

Half of the subjects responded with relative axial eye shortening after imposing positive defocus when they watched a movie with a foveal patch combined with an annular 6–9 deg eccentricity patch. However, on average, there was no significant difference between the defocused and control eyes at any time point of the experiment (20 min: +2 ± 14 μm vs. +6 ± 14 μm, 40 min: -2 ± 13 μm vs. +1 ± 15 μm, respectively, both n.s.) (Figs. 2 and 3D). The effect differed significantly from the effect of imposing full-field positive defocus (-2 ± 13 μm vs. -11 ± 12 μm, respectively, $p = 0.007$).

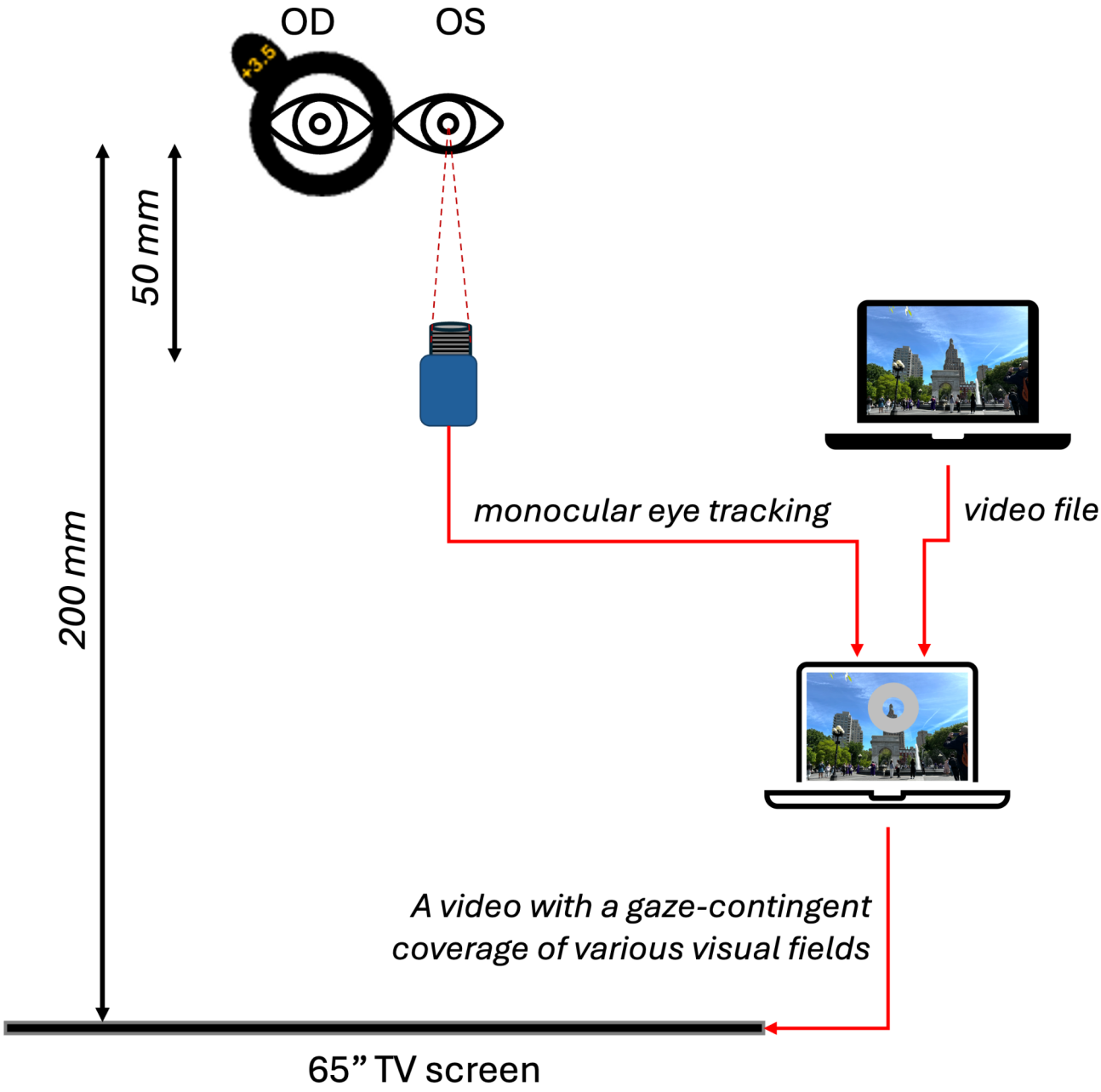

Fig. 4. Schematic illustration of experimental setup. Positive defocus was imposed monocularly in the right eye. The pupil of the left eye was tracked in infrared light (IR LEDs) with a custom-built eye tracker and custom-developed software to cover different parts of the movie frame in real-time with a gray patch while the subject watched a movie from a large TV screen at 2 m distance.

Effects of full-field patch with imposed defocus only on the area between 6 and 10 degrees eccentricity

Imposing positive defocus on only a small annular area between 6 and 10 degrees of retinal eccentricity induced significant eye shortening in exposed eyes after 20 and 40 min compared with control, fellow eyes (20 min: -6 ± 6 µm vs. 0 ± 8 µm, $p = 0.02$; 40 min: -9 ± 8 µm vs. -1 ± 8 µm, $p = 0.005$; respectively) and when compared to the baseline measurements (20 min: $p = 0.002$, 40 min: $p = 0.001$) (Figs. 2 and 3E). These changes were no different from those induced during the full-field defocus (20 min: -6 ± 9 µm vs. -10 ± 14 µm; 40 min: -9 ± 8 µm vs. -11 ± 12 µm, respectively, both n.s.) (Fig. 2).

Axial length changes in control, fellow eyes

There was no significant change in axial length in the control, fellow eyes under any of the experimental conditions (after 20 min: full-field: -3 ± 11 µm, patched fovea: -7 ± 14 µm, patched 3–9 deg eccentricity: +1 ± 10 µm, patched fovea combined with the annular patch of 6–9 deg eccentricity: +6 ± 14 µm; full-field patch with exposed only

6–10 deg eccentricity: 0 ± 8 µm; after 40 min: full-field: -1 ± 12 µm, patched fovea: -4 ± 9 µm, patched 3–9 deg eccentricity: +2 ± 14 µm, patched fovea combined with the annular patch of 6–9 deg eccentricity: +1 ± 15 µm, full-field patch with exposed only 6–10 deg eccentricity: -1 ± 8 µm; all n.s.). However, in some experimental conditions, especially the foveal patch, control eyes showed a similar temporal trend in axial length change as their defocused, fellow eyes. Possibly, changing retinal input by removing most of the visual cues from parts of the visual field could somewhat induce small changes in axial length even without the imposed defocus.

Discussion

In line with previous studies[6–8,10], we found that the foveal area provides only minor input to emmetropization and that the perifoveal region was most responsive to defocus. Moreover, we found that transient axial eye shortening induced by imposed positive defocus is absent when the retinal area between 3 and 9 deg eccentricity is covered with a gray patch. Panorgias et al. showed that the retina between 6 and 12 deg eccentricity is most sensitive to blur in their ERG recordings. In the current study, exposing an annular retinal area of 3 to 6 deg eccentricity and the retinal periphery beyond 9 deg eccentricity was not enough to evoke changes in axial length after 40 min of exposure to positive defocus. These observations suggested that the area between 6 and 9 deg eccentricity should be exposed to defocus as well to generate an effect on axial length. It is clear that the visual stimuli were different in both studies. Panorgias et al. used a stationary, phase-reversing DLS as a viewing target and measured the summed output of retinal activity by ERGs when parts of the stimulus were digitally low-pass filtered. Low-pass filtering by itself triggers axial eye elongation[29]. In the current study, positive optical defocus was imposed to induce axial eye shortening by activating "the inhibitory pathway of emmetropization"[29]. It is possible that the inhibitory and stimulatory mechanisms of emmetropization operate at slightly different retinal eccentricities. Also, animal studies in infant rhesus monkeys and chickens suggested that the peripheral retina, up to 20 degrees eccentricity, may be controlling emmetropization and possibly myopia development[9,30].

Since it is clear that the retinal location where positive defocus is introduced plays an important role, the question arises as to what differentiates the periphery from the central retina, and why is the fovea not as important. An obvious difference between the fovea and peripheral retina is the distribution of photoreceptors. The density of cone photoreceptors accounts to about 160.000 cones/mm^2 at 0 deg eccentricity, 14.000 cones/mm^2 at 6 deg, and 5.000 cones/mm^2 at 30 deg[31,32]. In contrast, the peak density of rod photoreceptors reaches 130.000 rods/mm^2 at 20 deg eccentricity and decreases markedly towards the fovea, with a density of approximately 60.000 rods/mm^2 at 5 deg, and a completely rod-free zone of 1.25 deg eccentricity[31,33,34]. Recent experiments in tree shrews[35] and human subjects[36] have shown that longitudinal chromatic aberration (LCA) may play a crucial role in emmetropization. Simulating LCA that is typical for a myopic eye (i.e. the blue plane is more blurred by chromatic defocus than the red) induced transient axial eye shortening in young adult human subjects already after 45 min[36]. To detect defocus in the blue end of the spectrum, S-cones ("blue cones") are needed. Since they are absent in the central 0.35 deg of the fovea[37,38], such a mechanism would not succeed in the fovea. However, S-cones are abundant in the periphery, with the highest density at approximately 1 deg eccentricity with a gradual decline until 20 deg[37,39]. Because S-cone density decreases less rapidly with eccentricity than overall cone density, the proportion of S-cones increases outside the fovea to a high level of 7.6% at 9 deg eccentricity[37]. Curcio et al. also showed that distances between S-cones and L- or M-cones are smaller than between L- and M-cones[37]. Visual acuity in the parafoveal S-cone system is around 5 cyc/deg which makes it possible to detect defocus below 1D, high enough to provide information on LCA for the control of eye growth[36]. Indeed, we found in the current study that imposing defocus on the retina only between 6 and 10 degrees eccentricity induced significant shortening of the axial length after 20 and 40 min which was similar to the changes induced by full-field defocus (Fig. 2). We propose that there may be a "sweet spot" for the control of emmetropization at a retinal eccentricity where the S-cone density provides a sensitive measure of chromatic defocus and the L- and M-cones are abundant enough to compare image defocus at long-wavelength end of the visible spectrum. The current study showed that the area around 6 and 10 deg eccentricity would be probably the most promising, although this may also vary among subjects. Note that 50% of tested eyes showed axial shortening when only the area between 3 and 6 degrees eccentricity and further periphery beyond 9 deg was exposed to positive defocus (Fig. 3D). Chui et al. described cone density as a function of refractive error and axial length and found that there was a decrease in cone density with increasing myopic refractive error and longer axial lengths[40]. Whether this was a result of retinal stretching associated with myopia development or a reason for emmetropization failure from the beginning requires more studies.

Our study also had some limitations. First, we tested only circular and annular gray patches around the fovea but there are other studies, showing that the superior retinal area may be most sensitive[41]. Second, we measured the induced changes in axial length in the fovea, while the stimulation occurred either full-field or only in the periphery. Current research (e.g[5,7,8]). as well as our experiment clearly showed that the periphery can control foveal eye growth and refraction. However, how the eye growth control signals are transmitted from the periphery to the center and from the retina to the choroid is still insufficiently understood and requires more experiments.

To summarize, we found that (1) foveal input is not needed to induce axial eye shortening with imposed positive defocus, (2) the retina cannot respond to imposed positive defocus when the retinal area between 3 and 9 degrees eccentricity is covered with a gray patch, (3) exposing the retinal area between 3 and 6 deg eccentricity and also beyond 9 deg had no average effect on axial length after 40 min, (4) since the effect of exposing retina only between 6 and 10 degrees eccentricity caused similar effects as full-field defocus, it may be that this area is a "sweet spot" for the detection of positive defocus.

Methods

Human subjects

Twenty young near-emmetropic adult (10 females, 28 ± 4 years of age) human subjects were enrolled in the study. Noncycloplegic refractions were confirmed in all participants by a commercial photorefractor (plusoptiX A12R, PlusOptix, Nürnberg, Germany). The average spherical equivalent (SE) of right eyes was 0.00 ± 0.63 diopters (D) and left eyes − 0.04 ± 0.76 D. The average anisometropia was 0.39 ± 0.40 D. None of the subjects needed optical correction for distance vision, had astigmatisms larger than 1 D or had previous ocular injuries. All subjects had normal binocular vision and correct vergence was verified with a custom-developed binocular eye tracker (see below and Supplementary Fig. S1). The study was conducted following the tenets of the Declaration of Helsinki and approved by the Swiss Research Ethics Committee (EKNZ, reference 2023 − 01503). Written informed consent was obtained from each subject before the experiments.

Study design and experimental setup

The study protocol included 5 appointments scheduled on 5 separate days, where subjects were asked to watch a movie by placing their head on a chinrest at a 2 m distance from the TV screen (65 inches, LG OLED65C9, 4 K, 2019). A custom-built infrared (IR) eye tracker (see details below) was placed in front of the subject's eyes at a 50 cm distance. The output data of the eye tracker were used to gaze-contingently cover parts of the movie frame with a grey patch (grey pixel values: $R = 127$, G = 127, B = 127) (Fig. 4). Additionally, an optical defocus of + 3.0 D was imposed by placing a + 3.5 D trial lens in front of the right eyes of the subjects during the entire experiment (a + 3.5D lens imposes 3D of myopic defocus when the eye is emmetropic and the viewing target is 2 m, or 0.5D, away). The optical defocus was imposed monocularly, while fellow eyes had sharp vision during the entire experiment and served as control.

To avoid possible confounding influences of the diurnal cycle, all appointments were scheduled at the same time of the day for each individual subject. The induced changes in axial length were measured with the ocular biometer Lenstar 900 with an autopositioning system (Haag-Streit, Switzerland) after 20 and 40 min of watching the movie during each appointment. Axial length was defined as the distance between the outer surface of the cornea and the RPE. Six repeated measurements of axial length were taken at each time point of the study from both eyes. Standard deviations did not exceed 10 µm. The effects of imposed defocus on axial length were investigated under four different visual field conditions: (1) full-field defocus, (2) a 3-deg eccentricity foveal patch (6 deg diameter), (3) a 3–9 deg eccentricity annular patch (6–18 deg diameter), and (4) a 3-deg eccentricity foveal patch combined with a 6–9 deg eccentricity annular patch (6 deg + 12–18 deg diameter) (Fig. 5A-C).

Fifteen out of twenty subjects were able to return and participate in an additional experiment that used the same experimental setup and design as described above experiment. To confirm that the near peripheral retina may be responsible for defocus detection, subjects watched a movie where only an area between 6 and 10 degrees eccentricity was exposed to the positive defocus, and a gray patch covered the rest of the image (Fig. 5D). This experiment was performed on a separate day, at the same time of the day as each individual subject performed previous experimental conditions.

Monocular eye tracking

The position of the left eye was tracked with an infrared (IR) monochrome camera (DMK37AUX287, Imaging Source, Germany) equipped with a 50 mm camera lens (Ricoh, Vietnam), a 50 mm infrared filter (Schneider, Kreuznach, Germany), and a set of sixteen IR (875 nm) light emitting diodes (LED) that were arranged in a

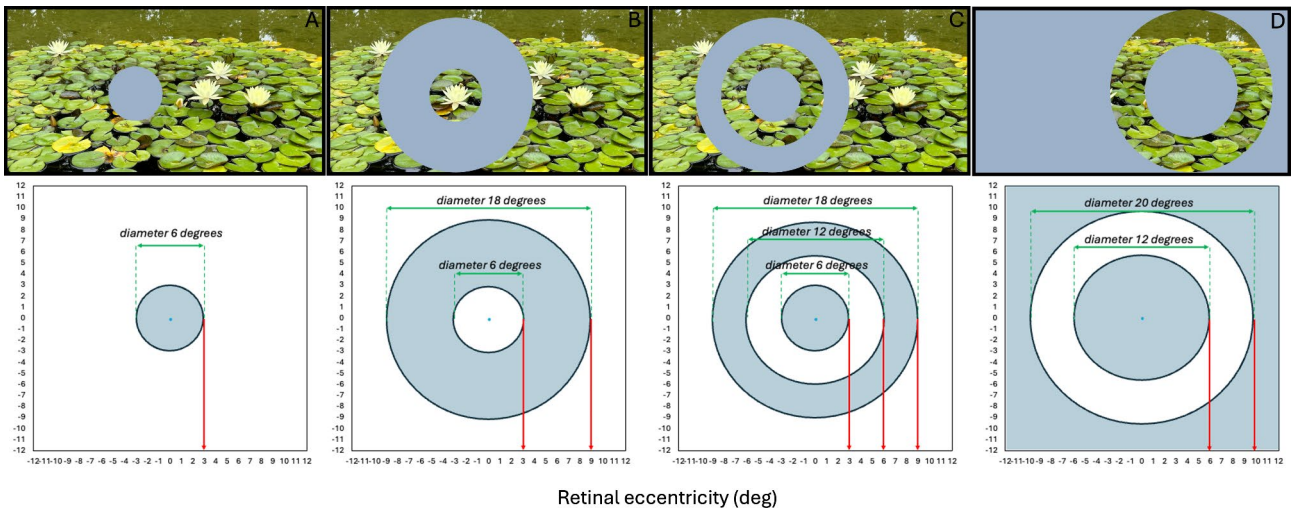

Fig. 5. Appearance of the movies with the gray patches, illustrated to scale. (**A**) 3 deg eccentricity foveal patch (6 deg diameter), (**B**) 3-9 deg eccentricity annular patch (diameter between 6 and 18 deg), (**C**) 3 deg eccentricity foveal patch combined with a 6-9 deg eccentricity annular patch (6 deg + 12-18 deg diameter), and (**D**) full-field patch where only annular area between 6 and 10 deg eccentricity exposed to positive defocus.

circular area with 40 mm diameter, fixed below the camera lens (Fig. 5). Custom-developed software written in Visual C++8.0 merged two inputs: (1) a video frame from the eye tracker camera (Y800, 640×480, camera output at 160 Hz), and (2) a video frame with a movie (RGB24, 1920×1080, 60 Hz). The pupil of the left eye and the first Purkinje image were tracked to record the fixation points after calibration. The calibration procedure required the subjects to fixate 4 points on the screen in sequence which appeared one after the other as soon as the software had identified fixation. Fixation was detected by the software based on a drop in the running standard deviations of eye positions below 0.2 degrees. The calibration of the eye tracker was done for each subject before and after each 10 min of the experiment to ensure that eye positions remained correctly measured. Each calibration took a maximum of 10 s. The time lag between eye position measurements and the position of the patches on the screen was 1/60 sec and was not visible (author's observation).

Binocular eye tracking setup

To ensure that all subjects had normal binocular vision and eyes convergence, an additional experiment was done before they were enrolled in the study. We used a custom-built binocular eye tracker that was previously described[28]. It consisted of two infrared (IR) sensitive monochrome cameras (DMK 37AUX287, Imaging Source, Germany), equipped with two 50 mm camera lenses (Ricoh, Vietnam), that were covered with 50 mm infrared filters (Schneider, Kreuznach, Germany). The output of both cameras was merged in one frame buffer and processed by the same program. Both pupils and their first Purkinje images were tracked. Purkinje images were generated by a circular array of 16 IR LEDs with 40 mm diameter, fixed in the middle below both cameras. Calibration was done simultaneously for both eyes, and both cameras were used at a frame rate of 500 Hz.

Statistics

All statistical analysis and two-dimensional density plots were performed using a free software environment R (version 4.2.2., R Foundation for Statistical Computing, Vienna, Austria). The normality of the data was confirmed with a Shapiro-Wilk test. The significance of the changes induced in axial length was calculated using a repeated measures analysis of variance (ANOVA) with two within-subject factors of time and visual field patching condition, followed by a post hoc test with Bonferroni correction.

Data availability

The datasets used during the current study are available from the corresponding author at a reasonable request (Dr. Barbara Swiatczak barbaraswiatczak@gmail.com).

Received: 9 July 2024; Accepted: 29 October 2024
Published online: 05 November 2024

References

1. Erdinest, N. et al. Peripheral defocus and myopia management: A mini-review. *Korean J. Ophthalmol.* **37**, 70–81. https://doi.org/10.3341/kjo.2022.0125 (2023).
2. Wallman, J. & Winawer, J. Homeostasis of eye growth and the question of myopia. *Neuron*. **43**, 447–468. https://doi.org/10.1016/j.neuron.2004.08.008 (2004).
3. Smith, E. L. Prentice Award Lecture 2010: A case for peripheral optical treatment strategies for myopia. *Optom Vis Sci.* **88**, 1029–1044. https://doi.org/10.1097/OPX.0b013e3182279cfa (2011).
4. Diether, S. & Schaeffel, F. Local changes in eye growth induced by imposed local refractive error despite active accommodation. *Vis. Res.* **37**, 659–668. https://doi.org/10.1016/s0042-6989(96)00224-6 (1997).
5. Smith, E. L., Kee, C. S., Ramamirtham, R., Qiao-Grider, Y. & Hung, L. F. Peripheral vision can influence eye growth and refractive development in infant monkeys. *Invest. Ophthalmol. Vis. Sci.* **46**, 3965–3972. https://doi.org/10.1167/iovs.05-0445 (2005).
6. Smith, E. L. et al. Effects of foveal ablation on emmetropization and form-deprivation myopia. *Invest. Ophthalmol. Vis. Sci.* **48**, 3914–3922. https://doi.org/10.1167/iovs.06-1264 (2007).
7. Huang, J., Hung, L. F. & Smith, E. L. Effects of foveal ablation on the pattern of peripheral refractive errors in normal and form-deprived infant rhesus monkeys (Macaca mulatta). *Invest. Ophthalmol. Vis. Sci.* **52**, 6428–6434. https://doi.org/10.1167/iovs.10-6757 (2011).
8. Benavente-Pérez, A., Nour, A. & Troilo, D. Axial eye growth and refractive error development can be modified by exposing the peripheral retina to relative myopic or hyperopic defocus. *Invest. Ophthalmol. Vis. Sci.* **55**, 6765–6773. https://doi.org/10.1167/iovs.14-14524 (2014).
9. Smith Iii, E. L. et al. Eccentricity-dependent effects of simultaneous competing defocus on emmetropization in infant rhesus monkeys. *Vis. Res.* **177**, 32–40. https://doi.org/10.1016/j.visres.2020.08.003 (2020).
10. Panorgias, A. et al. Retinal responses to simulated optical blur using a novel dead leaves ERG stimulus. *Invest. Ophthalmol. Vis. Sci.* **62**, 1. https://doi.org/10.1167/iovs.62.10.1 (2021).
11. Lam, C. S. Y. et al. Defocus incorporated multiple segments (DIMS) spectacle lenses slow myopia progression: A 2-year randomised clinical trial. *Br. J. Ophthalmol.* **104**, 363–368. https://doi.org/10.1136/bjophthalmol-2018-313739 (2020).
12. Bao, J. et al. Spectacle lenses with aspherical lenslets for myopia control vs single-vision spectacle lenses: A randomized clinical trial. *JAMA Ophthalmol.* **140**, 472–478. https://doi.org/10.1001/jamaophthalmol.2022.0401 (2022).
13. Mutti, D. O. et al. Refractive error, axial length, and relative peripheral refractive error before and after the onset of myopia. *Invest. Ophthalmol. Vis. Sci.* **48**, 2510–2519. https://doi.org/10.1167/iovs.06-0562 (2007).
14. Sng, C. C. et al. Change in peripheral refraction over time in Singapore Chinese children. *Invest. Ophthalmol. Vis. Sci.* **52**, 7880–7887. https://doi.org/10.1167/iovs.11-7290 (2011).
15. Seidemann, A., Schaeffel, F., Guirao, A., Lopez-Gil, N. & Artal, P. Peripheral refractive errors in myopic, emmetropic, and hyperopic young subjects. *J. Opt. Soc. Am. Opt. Image Sci. Vis.* **19**, 2363–2373. https://doi.org/10.1364/josaa.19.002363 (2002).
16. Atchison, D. A. & Charman, W. N. Optics of spectacle lenses intended to treat myopia progression. *Optom. Vis. Sci.* **101**, 238–249. https://doi.org/10.1097/OPX.0000000000002140 (2024).
17. Lam, C. S. et al. Myopia control effect of Defocus incorporated multiple segments (DIMS) spectacle lens in Chinese children: results of a 3-year follow-up study. *Br. J. Ophthalmol.* **106**, 1110–1114. https://doi.org/10.1136/bjophthalmol-2020-317664 (2022).
18. Chalberg, T. et al. Control of myopia using Diffusion Optics spectacle lenses: Efficacy and Safety Study (CYPRESS) 42-month results. *Invest. Ophthalmol. Vis. Sci.* **64**, 5092 (2023).

19. Rappon, J. et al. Control of myopia using diffusion optics spectacle lenses: 12-month results of a randomised controlled, efficacy and safety study (CYPRESS). *Br. J. Ophthalmol.* **107**, 1709–1715. https://doi.org/10.1136/bjo-2021-321005 (2023).
20. Li, X. et al. Myopia control efficacy of spectacle lenses with aspherical lenslets: Results of a 3-year follow-up study. *Am. J. Ophthalmol.* **253**, 160–168. https://doi.org/10.1016/j.ajo.2023.03.030 (2023).
21. Sanchez-Tena, C. A. P. M. A., Villa-Collar, C., Martinez-Perez, C., Padmaja, S. & Ohlendorf, A. Efficacy of a next-generation design of ophthalmic lenses for myopia control: Six-month results of the CEME study. *Invest. Ophthalmol. Vis. Sci.* **65**(7), 133 (2024).
22. Muhiddin, H. S. et al. Choroidal thickness in correlation with axial length and myopia degree. *Vis. (Basel).* **6**. https://doi.org/10.3390/vision6010016 (2022).
23. Wu, H. et al. Short-term choroidal changes as early indicators for future myopic shift in primary school children: Results of a 2-year cohort study. *Br. J. Ophthalmol.* **325871** https://doi.org/10.1136/bjo-2024-325871 (2024).
24. Liu, M. et al. Dynamic changes of choroidal vasculature and its association with myopia control efficacy in children during 1-year orthokeratology treatment. *Cont. Lens Anterior Eye.* **102314** https://doi.org/10.1016/j.clae.2024.102314 (2024).
25. Winawer, J. & Wallman, J. Temporal constraints on lens compensation in chicks. *Vis. Res.* **42**, 2651–2668. https://doi.org/10.1016/s0042-6989(02)00300-0 (2002).
26. Wang, D. et al. Optical Defocus rapidly changes Choroidal Thickness in Schoolchildren. *PLoS One.* **11**, e0161535. https://doi.org/10.1371/journal.pone.0161535 (2016).
27. Read, S. A., Collins, M. J. & Sander, B. P. Human optical axial length and defocus. *Invest. Ophthalmol. Vis. Sci.* **51**, 6262–6269. https://doi.org/10.1167/iovs.10-5457 (2010).
28. Ivanchenko, D., Rifai, K., Hafed, Z. M. & Schaeffel, F. A low-cost, high-performance video-based binocular eye tracker for psychophysical research. *J. Eye Mov. Res.* **14** https://doi.org/10.16910/jemr.14.3.3 (2021).
29. Schaeffel, F. & Swiatczak, B. Mechanisms of emmetropization and what might go wrong in myopia. *Vis. Res.* **220**, 108402. https://doi.org/10.1016/j.visres.2024.108402 (2024).
30. Liu, Y. & Wildsoet, C. The effect of two-zone concentric bifocal spectacle lenses on refractive error development and eye growth in young chicks. *Invest. Ophthalmol. Vis. Sci.* **52**, 1078–1086. https://doi.org/10.1167/iovs.10-5716 (2011).
31. Curcio, C. A., Sloan, K. R., Kalina, R. E. & Hendrickson, A. E. Human photoreceptor topography. *J. Comp. Neurol.* **292**, 497–523. https://doi.org/10.1002/cne.902920402 (1990).
32. Song, H., Chui, T. Y., Zhong, Z., Elsner, A. E. & Burns, S. A. Variation of cone photoreceptor packing density with retinal eccentricity and age. *Invest. Ophthalmol. Vis. Sci.* **52**, 7376–7384. https://doi.org/10.1167/iovs.11-7199 (2011).
33. Lee, S. C. S., Martin, P. R. & Grünert, U. Topography of neurons in the rod pathway of human retina. *Invest. Ophthalmol. Vis. Sci.* **60**, 2848–2859. https://doi.org/10.1167/iovs.19-27217 (2019).
34. Wells-Gray, E. M., Choi, S. S., Bries, A. & Doble, N. Variation in rod and cone density from the fovea to the mid-periphery in healthy human retinas using adaptive optics scanning laser ophthalmoscopy. *Eye (Lond).* **30**, 1135–1143. https://doi.org/10.1038/eye.2016.107 (2016).
35. Gawne, T. J., She, Z. & Norton, T. T. Chromatically simulated myopic blur counteracts a myopiagenic environment. *Exp. Eye Res.* **222**, 109187. https://doi.org/10.1016/j.exer.2022.109187 (2022).
36. Swiatczak, B. & Schaeffel, F. Myopia: Why the retina stops inhibiting eye growth. *Sci. Rep.* **12**, 21704. https://doi.org/10.1038/s41598-022-26323-7 (2022).
37. Curcio, C. A. et al. Distribution and morphology of human cone photoreceptors stained with anti-blue opsin. *J. Comp. Neurol.* **312**, 610–624. https://doi.org/10.1002/cne.903120411 (1991).
38. Chen, Y., Lan, W. & Schaeffel, F. Size of the foveal blue scotoma related to the shape of the foveal pit but not to macular pigment. *Vis. Res.* **106**, 81–89. https://doi.org/10.1016/j.visres.2014.10.011 (2015).
39. Ahnelt, P. K. The photoreceptor mosaic. *Eye (Lond).* (Pt 3b), 12. https://doi.org/10.1038/eye.1998.142 (1998).
40. Chui, T. Y., Song, H. & Burns, S. A. Individual variations in human cone photoreceptor packing density: Variations with refractive error. *Invest. Ophthalmol. Vis. Sci.* **49**, 4679–4687. https://doi.org/10.1167/iovs.08-2135 (2008).
41. Lin, Z. et al. Relative myopic defocus in the superior retina as an indicator of myopia development in children. *Invest. Ophthalmol. Vis. Sci.* **64**, 16. https://doi.org/10.1167/iovs.64.4.16 (2023).

Acknowledgements

We would like to thank Dr. Torsten Strasser, Ophthalmic Research Institute, University of Tübingen, Germany for his initial help to merge the movie video signal and the eye tracker video in one video buffer, as well as Pfizer Switzerland and Swiss Vitreoretinal Group for supporting our research.

Author contributions

B.S.: experimental design, programming, measurements, data analysis, statistics, figures, writing; H.S.: data inspection, manuscript revision; F.S.: programming, experimental design, data inspection, writing.

Funding

The project was funded by the Institute of Molecular and Clinical Ophthalmology (IOB) in Basel, Switzerland, and the Swiss RetinAward 2023 to Barbara Swiatczak.

Declarations

Competing interests

The authors declare no competing interests.

Additional information

Supplementary Information The online version contains supplementary material available at https://doi.org/10.1038/s41598-024-78300-x.

Correspondence and requests for materials should be addressed to B.S.